is the stretching factor of the vortex line at the given material point.

It may be worth noting that if we introduce a small material cylinder (around an element $d\boldsymbol{x}$ of a vortex line) having a cross section dA and a constant mass

$$dm = \rho dA\,|d\boldsymbol{x}| = \rho_0 dA_0\,|d\boldsymbol{x}|_0 \tag{20}$$

one obtains, using Eqs. (19) and (20),

$$|\omega|\,dA = |\boldsymbol{\omega}_0|\,dA_0 \tag{21}$$

in agreement with Kelvin's theorem, which states that $d\Gamma/dt = 0$, with

$$\Gamma = \oint_C \boldsymbol{v}\cdot d\boldsymbol{x} = \int\int_\sigma \boldsymbol{\omega}\cdot\boldsymbol{n}\,d\sigma \tag{22}$$

where C is a material contour and σ any surface with C as its boundary.

Computational Applications

The above results also have important computational applications. Consider for simplicity the case of an inviscid and isentropic flow (e.g., as indicated above, the case in which viscosity and conductivity are negligible and the flowfield is isentropic at time t = 0). In this case the vorticity is given by Eq. (13) at all times. Assume that we know the vorticity field at time $t = t_0$ and the functions $\boldsymbol{x}(\xi^\alpha, t)$ at times t, and t_1. Whereas these pieces of information are not sufficient to evaluate the velocity field, nonetheless they are sufficient to evaluate the vorticity field at time t_1. Indeed, from $\boldsymbol{x}(\xi^\alpha, t_0)$ we may evaluate the vectors $\boldsymbol{g}_\beta$ at $t = t_0$ and hence the contravariant components $\omega^\beta(\xi^\alpha, t_0)$ as well as $J(\xi^\alpha, t_0)$. On the other hand, the knowledge of $\boldsymbol{x}(\xi^\alpha, t_1)$ (which may be obtained with the procedure outlined below), allows for the evaluation of $\boldsymbol{g}_\beta$ and J at $t = t_1$ and hence of the vorticity field, via Eq. (14).

Therefore, Eq. (14), besides its theoretical applications, may be exploited for computational purposes. For instance, consider the particularly complex problem of wake dynamics for a helicopter rotor is an incompressible flow. For this problem the vorticity is concentrated in the boundary layer and the wake. Within the wake the flow may be treated as inviscid.[5] Once the locations of material grid points are evaluated at a given time step, the direction and intensity of the vorticity field can be evaluated immediately using Eq. (14) [or the simpler Eq. (17) if the points of the grid are initially aligned with the vortical lines]. Once the vorticity is known, the velocity is evaluated using the Biot-Savart law (with the addition of the gradient of a scalar potential to satisfy normal boundary conditions; see Ref. 6 for details). This provides an extension to distributed vorticity of the formulation introduced in Ref. 5 for potential flows. In general, if the assumption of inviscid isentropic flow is not adequate, ω^α may be evaluated, step by step, using Eq. (16).

Conclusions

In summary, Cauchy's classical result given by Eq. (15) has been reinterpreted in terms of contravariant components in a material curvilinear coordinate system. Also, Vaszonyi's vorticity equation was extended to viscous flows and Cauchy's result was extended to such flows [Eq. (16)]. The elimination of the unnecessary constraint that the ξ^α coordinates coincide, at $t = 0$, with the Cartesian components has facilitated the derivation of classical vortex theorems. The use of the results for the computational solution of the generalized vorticity equation was also outlined.

Acknowledgments

This work was supported by the Army Research Office (Contract No. DAAG26-83-K-0050 to Boston University). The author wishes to thank Dr. Guido Sandri and Dr. Norman D. Zabusky for their encouragement and recommendations on the writing of this Note.

References

[1] Serrin, J., "Mathematical Principles of Classical Fluid Mechanics," *Encyclopedia of Physics*, edited by S. Flugge, Vol. VIII/1, *Fluid Dynamics I*, coedited by C. Truesdell, Springer-Verlag, Berlin, 1959, pp. 125-263.

[2] Sokolnikoff, I.S., *Tensor Analysis*, 2nd Ed., John Wiley & Sons, New York, 1964.

[3] Morino, L., "A Finite-Element Method for Rotational Incompressible Aerodynamics," Boston University, College of Engineering, TN-74-04, Dec. 1974.

[4] Morino, L., "A General Scalar/Vector Potential Formulation for Compressible Viscous Unsteady Flows," ICARUS, Boston, TR-84-01, Aug. 1984.

[5] Morino, L., Kaprielian, Z. Jr., and Sipcic, S.R., "Free Wake Analysis of Helicopter Rotors," *Vertica*, Vol. 9, June/July 1985.

[6] Morino, L. and Bharadvaj, B., "Two Methods for the Free Wake Analysis of Helicopter Rotors," Boston University Center for Computational and Applied Dynamics, TR-85-02, Aug. 1985.

Turbulent Boundary Layers with Vectored Mass Transfer

Gustave J. Hokenson*
The Hokenson Company, Los Angeles, California

THE excellent data presented in Ref. 1 provide substantial guidance in the understanding of many of the subtleties of turbulent boundary-layer (TBL) flows with blowing, and the modeling thereof. In an effort to peel away quantitatively the various interacting elements of the flow, it is proposed that the following approach may be useful for exploiting such data in model development. If the Reynolds-averaged equations of motion are further locally spatially averaged in horizontal planes, with a scale large relative to the porosity yet small relative to the boundary-layer growth, the discrete jet blowing may be converted into its distributed mass transfer equivalent. For example,

$$\bar{u} = \langle \bar{u} \rangle + \bar{u}^\circ \tag{1}$$

where $\bar{u}$ is the time-averaged streamwise velocity and $\langle\ \rangle$, $(\ )^\circ$ denote the local spatial average and the variation therefrom, respectively. As a result of this local spatial averaging, the governing equation nonlinearities generate extra (Reynolds stress-like) terms due to the spatial variations. (Note that a piecewise constant filter function is used such that no Leonard terms appear.) In addition, the average normal velocity at the surface is now simply related to the total flow rate and area, which reduces the local jet-like values of wall normal velocity by the open area ratio of the surface, while the average skin friction is the weighted sum of the solid surface plus open surface contributions. Finally, the doubly averaged streamwise velocity and turbulence at the wall are now nonzero.

It appears that the location in the boundary layer at which $\langle \bar{u}^\circ \bar{v}^\circ \rangle \simeq 0$ (where v is the time-averaged normal velocity) defines a level that divides the relatively weakly sheared

Received June 3, 1985.

*Chief Scientist. Member AIAA.

outer flow, which is readily characterizable from even linear theory,, from an inner flow where the $\langle \tilde{u}^\circ \tilde{v}^\circ \rangle$ decay results from the discrete jet mixing and streamwise deflection. Given some relationship between $\langle \tilde{u} \rangle_w$, $\langle \tilde{u}^\circ \tilde{v}^\circ \rangle_w$, $\langle \overline{u'v'} \rangle_w$, and the wall structure (where $'$ denotes turbulent fluctuations and w wall conditions), the inner layer typified by high shear, relatively low speed flow may also be characterizable.[3]

In a constant pressure integral formulation (which may be most convenient for data analysis), the aforementioned phenomena may be expressed:

$$\frac{d\theta}{dx} = \left(1 - \frac{\langle \tilde{u} \rangle_w}{u_e}\right)\frac{\langle \tilde{v} \rangle_w}{u_e} - \frac{\langle \tilde{u}^\circ \tilde{v}^\circ \rangle_w}{u_e^2} - \frac{\langle \overline{u'v'} \rangle_w}{u_e^2} + \frac{C_f}{2} \quad (2)$$

where θ is the momentum thickness, C_f the skin friction coefficient, u_e the freestream velocity, and the additional terms correspond to the three effects discussed here, $\langle \tilde{u}^{\circ 2} \rangle_{,x}$ having been deleted. The modeling problem that the data in Ref. 1 should significantly impact is twofold:

1) $(\tilde{u})_{,,}$ $\langle \tilde{u}^\circ \tilde{v}^\circ \rangle_w$, and $\langle \overline{u'v'} \rangle_w$ all depend on the details of the flow through the particular wall. Although $\langle \tilde{u} \rangle_w$ and $\langle \overline{u'v'} \rangle_w$ may be estimated from the data, $\langle \tilde{u}^\circ \tilde{v}^\circ \rangle_w$ must be treated parametrically until a compatible solution is obtained.

2) As in all TBL modeling, C_f depends explicitly on all other effects on the right-hand side of the equation.

Therefore, some effort is required to assess which effects are important and their quantitative contribution in a general case.

Due to the relatively low blowing rates used in Ref. 1 (relative to that which would cause separation), both the vectoring effect $\langle \tilde{u} \rangle_w$ and the explicit dependence of C_f on the mass transfer may be ignored in this particular case. The resulting error of a few percent is well within the precision of the data. This allows us to focus on the representation of the terms

$$-\langle \tilde{u}^\circ \tilde{v}^\circ \rangle_w / u_e^2 - \langle \overline{u'v'} \rangle_w / u_e^2 \quad (3)$$

which are herein combined into the following single modeling expression

$$C_1 + C_2 b^2 \quad (4)$$

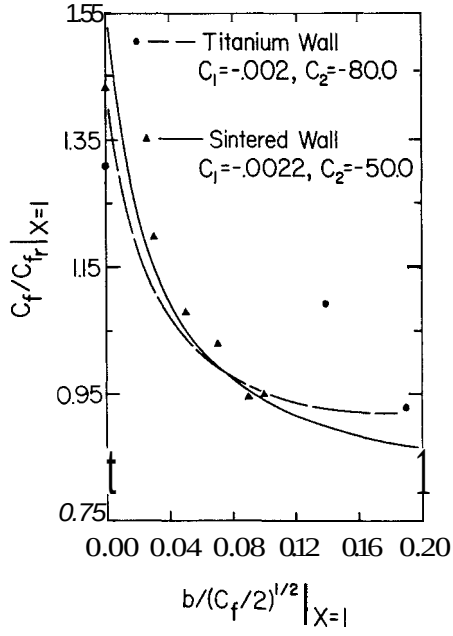

Fig. 1 Comparison between the experimental data of Ref. 1 and the modeling of Eq. (3) by Eq. (4).

where

$$b \equiv \langle v \rangle_w / u_e \quad (5)$$

By systematically varying the constants C_1 and C_2, the data may be fit reasonably well with $C_1 = 0.002$ and $C_2 = -80.0$ for the titanium wall, whereas $C_1 = -0.0022$ and $C_2 = -50.0$ are indicated for the sintered wall, as shown in Fig. 1. Clearly, C_1 scales with C_f and C_2 scales with $C_f^{-1/2}$, implying that the friction velocity is the appropriate reference. Note that, since the coefficients are negative, it is evident that the effect of $-\langle \tilde{u}^\circ \tilde{v}^\circ \rangle_w$ is dominant since we expect $-\langle \overline{u'v'} \rangle_w$ to be positive.

If this functional dependence persists, analysis suggests that a rise in the measured C_f is possible, over a range of larger b values than used in Ref. 1, prior to a falloff at still higher mass transfer rates. It also should be mentioned that, in measurements of forces on such a porous plate, the drag would reflect only the solid surface portion of the C_f in this form of the boundary-layer equations. However, the measured force would include a pressure difference within the passages of the porous wall due to the $\dot{m}\langle \tilde{u} \rangle_w$ vectoring (seen in the boundary-layer equation), which also involves the contribution to C_f averaging from the open surface.

For cases in which the induced mass transfer vectoring, and $(U)_w$, is significant, angle (a)magnitude (m) variables may be appropriate. Utilizing the following definitions of a, m:

$$\alpha \equiv \langle \tilde{v} \rangle_w / \langle \tilde{u} \rangle_w \quad (6)$$

$$m \equiv (1+\alpha^2)^{1/2} \langle u \rangle_w / u_e \quad (7)$$

the vectored blowing term in the boundary-layer equation becomes

$$[m^2 - m(1+\alpha^2)^{1/2}]\,[-\alpha/(1+\alpha^2)] \quad (8)$$

The magnitude m responds to the pressure difference across the porous surface and its "loss coefficient," whereas α provides a sensitive measure of the induced vectoring, which also depends on the flow within the porous wall through $\langle \tilde{u}^\circ \tilde{v}^\circ \rangle_w$ and $\langle \overline{u'v'} \rangle_w$. The mass transfer term in this form exhibits extrema with which the effect of vectoring may be evaluated. For a given a, this term exhibits an extremum when $\langle \tilde{u} \rangle_w / u_e = 1/2$ and, for a given m, when $\langle \tilde{u} \rangle_w / u_e = (1 \pm (1+8m^2)^{1/2})/4 \simeq -m^2,\ 1/2 + m^2$. Since $\langle \tilde{u} \rangle_w$ will be >0 yet $\ll 1/2$, the effect of naturally induced vectoring could be relatively small. The effect of actively imposed optimal mass transfer vectoring is currently being studied for both steady and unsteady flows and will be the subject of a future paper.

Acknowledgment

This work was carried out under the sponsorship of the Aerospace Sciences Directorate, AFOSR and the Office of Basic Energy Sciences, Department of Energy.

References

[1]Collier, F. S. Jr. and Schetz, J. A., "Injection into a Turbulent Boundary Layer Through Different Porous Surfaces," ***AIAA Journal,*** Vol. 22, June 1984, pp. 839-891.

[2]Hokenson, G. J., "Linearized k-ϵ Analysis of Free Turbulent Mixing in Streamwise Pressure Gradients with Experimental Verification," ***Journal of Applied Mechanics,*** Vol. 46, No. 3, Sept. 1979, pp. 493-498.

[3]Hokenson, G. J., "Boundary Conditions for Flow Over Permeable Surfaces," ***Journal of Fluids Engineering,*** Vol. 107, No. 3, Sept. 1985, pp. 430-432.